

Protoclusters of galaxies and overdensities of star-forming galaxies: the case of MRC1138-26 - the Spiderweb



Ivan Valtchanov (1), B. Altieri (1), S. Berta (2), E. Chapin (3), D. Coia (1), L. Conversi (1), H. Dannerbauer (4), H. Domínguez-Sánchez (5,6), T.D. Rawle (1), M. Sánchez-Portal (1), J.S. Santos (1), S. Tempurin (7), J. Kurk (2)

(1) Herschel Science Centre, ESAC, ESA; (2) MPE, Garching, Germany; (3) XMM-SOC, ESAC, ESA; (4) U. Wien, Austria; (5) IAC, Spain; (6) U. La Laguna, Spain; (7) U. Innsbruck, Austria;

Introduction

- Today's (z<1) massive clusters of galaxies are made of passive "red and dead" galaxies. Going to earlier times the fraction of star-forming galaxies in dense regions increases (eg Elbaz+07; Popesso+12). The SFR density peaks at z=2-3 (Hopkins & Beacom 06), but we cannot talk about clusters (from an observational point of view) as they are still forming and not yet in shape to be easily detected (eg if virialized).
- Different signposts are used as tracers of these protoclusters: powerful radio galaxies and QSOs (see Miley & De Breuck 2008 for a review) or submm detected (SMGs) galaxies (eg Chapman+09).
- To confirm a protocluster a number density excess of galaxies at a similar redshift to the radio galaxy/QSO or SMG is reported: galaxies identified using Ly α /Ha or other rest-frame UV or optical lines (Kurk+04a,b; Koyama+13), narrow band imaging or NIR/colour selections (eg Hatch+11), submm imaging (Stevens+10).
- The high redshift and the foreground/background contamination make the search for protoclusters in broad bands impossible task, if there is no colour information, spectroscopy or accurate photometric redshift. None of the protoclusters known to date can be **visually** identified in a broad band map from *Spitzer* or other ground-based or space facilities.
- Overdensities of star-forming galaxies in broad-band maps should exist, based on the physically motivated framework (e.g. Granato+04; Lapi+11; Cai+13) and the predictions from the clustering and the number counts (Negrello+05).
- The SFR density peaks at z=2-3 (eg Hopkins & Beacom 06) and then declines strongly at smaller redshift. For galaxies falling in a dark matter halo of a protocluster the star-burst episodes occur at the same epoch (Granato+04).
- The SED peak of a dusty star-forming galaxy (DSFGs) is at $\sim 100 \mu\text{m}$ rest-frame ($\sim 300 \mu\text{m}$ at z=2). So, Herschel/SPiRE is the best instrument to search for overdensities of DSFGs as it can quickly map down to the confusion limit large areas in three broad bands: 250, 350 and 500 μm .
- Planck is also well matched to search for overdensities (see Negrello+05) although it will be necessary to follow them up with Herschel and/or deep NIR imaging (see Clements+13) because of the large Planck beam and the degeneracy of source type with the emission at Planck wavelengths (eg clumps of dusty sources or synchrotron emission or nearby galaxies).
- Protocluster fields, especially those around the peak of the SFR density, are the natural location to search for such overdensities.

The Spiderweb protocluster

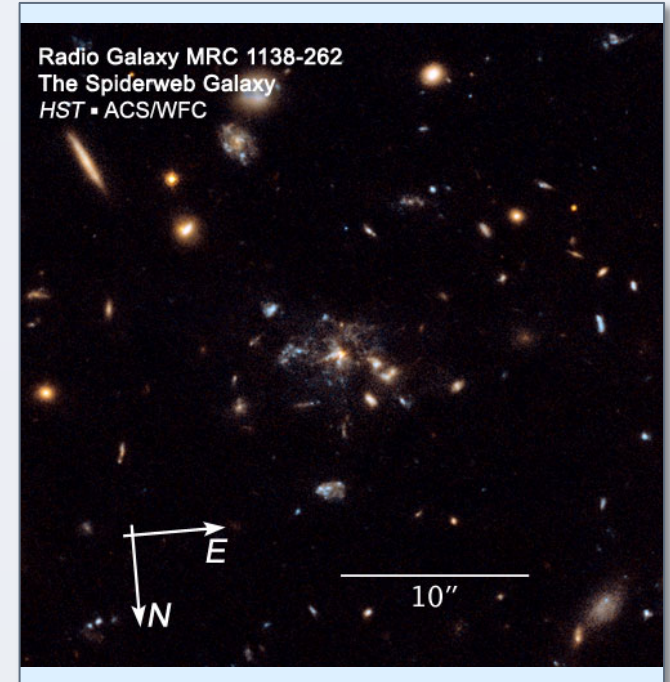


Fig.1 The Spiderweb radio galaxy.

Also known as PKS1138-262 (or MRC1138-262) is one of the best studied protoclusters. The central radio galaxy, the "hungry" spider is at redshift z=2.16 and form stars with a rate of $\sim 1400 M_{\odot}/\text{year}$ (see Seymour+12). Significant number density excess of galaxies emitting Ly α and Ha or having NIR colours consistent with the 400 nm break at z=2.2 are reported (see eg Koyama+13 for a recent overview and references therein). A large-scale filament (10 Mpc comoving size) is also reported (Koyama+13).

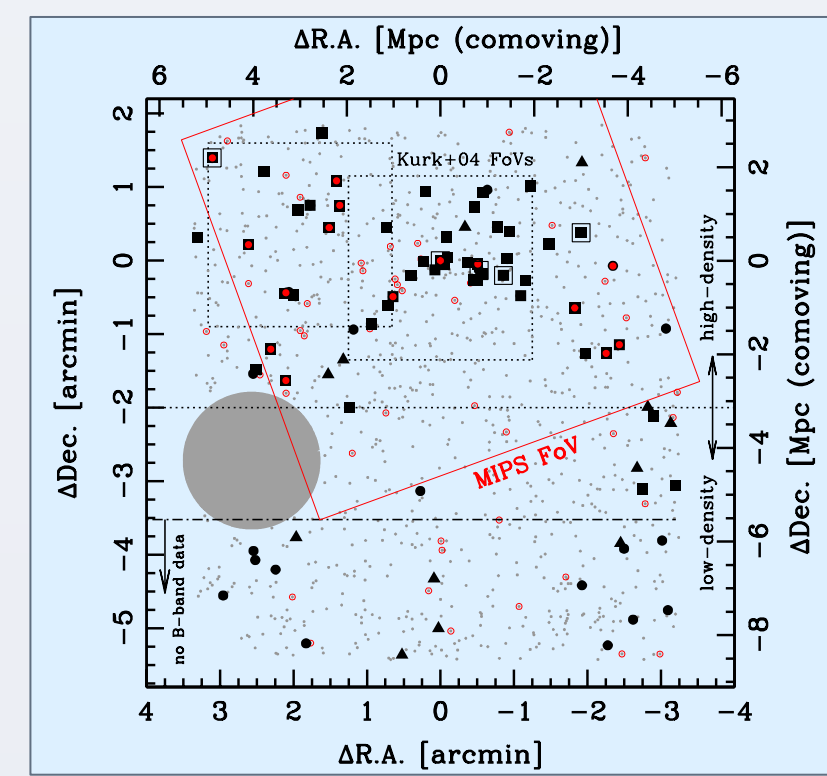


Fig.2 (taken from Koyama+13) showing the Spiderweb field and the available observations. H α +BzK (black squares), H α -BzK (black circles), H α -Ks (black triangles), distant red galaxies (red circles).

Herschel observations and data processing

- Herschel PACS and SPiRE imaging as part of the HSC guaranteed time (PI B. Altieri).
- PACS maps at 100 μm and 160 μm cover only $\sim 5' \times 5'$ around the radio galaxy.
- SPiRE maps in 250, 350 and 500 μm cover larger region: $\sim 20'$ radius, down to the extragalactic confusion noise. There are also OT1 SPiRE observations (PI H. Röttgering) covering even larger field (see Rigby+13).
- Standard SPiRE map making with HIPE v10, using the destriper and also including the telescope turnaround data.
- SPiRE maps were shifted to match Spitzer/MIPS 24 μm astrometry (only in the centre).
- SPiRE maps depth: (6.8, 8.3, 7.6) mJy at (250, 350, 500) μm close to Nguyen+10 limits.
- SPiRE source detection: using Sussextractor (SXT, Smith+12). In the Spiderweb field we detect 817 sources in the SPiRE 250 μm map, above a signal-to-noise ratio of 3. There are 366 sources at relative coverage above 50%.
- SPiRE 250 μm sources are used as priors for the SXT run on 350 and 500 μm maps.
- SPiRE extragalactic control fields:
 - GOODS-North, Lockman, COSMOS and UDS from HerMES (see Oliver+12 for overview).
 - Trimmed down to the same depth (same map repetitions) and applying the same map making and source detection with SXT.

Overdensity of SPiRE 250 μm sources

Serendipitously identified as a visually compelling clump of a large number of 250 μm sources in the Spiderweb field: at $\sim 7'$ south of the radio galaxy (see Fig.1). Only SPiRE data available and shallow all sky survey data from WISE (Wright +10).

\Rightarrow To quantify it we make use of an adaptive kernel density estimate (AKDE, see Pisani96) and compare it with AKDE from fields of randomly distributed sources, as well as the AKDE results from the four control fields.

\Rightarrow Results:

- \Rightarrow AKDE peak is at 5.1σ with respect to the background
- \Rightarrow In 2 out of 100 fields of randomly distributed sources we detect similar or higher significance AKDE peak (range is from 3.6 to 5.4σ). We do not check the size \Rightarrow the 2% is an upper limit.
- \Rightarrow No AKDE peak at similar contrast in the control fields, the max AKDE of 4.9σ is in Lockman. None of the AKDE regions above 3σ can be linked to known protoclusters.
- \Rightarrow Definition of the overdensity: AKDE peaks at (11:41:04.44, -26:35:08.6, J2000.0), size $\sim 3.5'$ (3σ contours). For the analysis we use slightly offset centre (11:40:59.5, -26:35:11) and radius of $4'$ (the red circle in Fig.1).

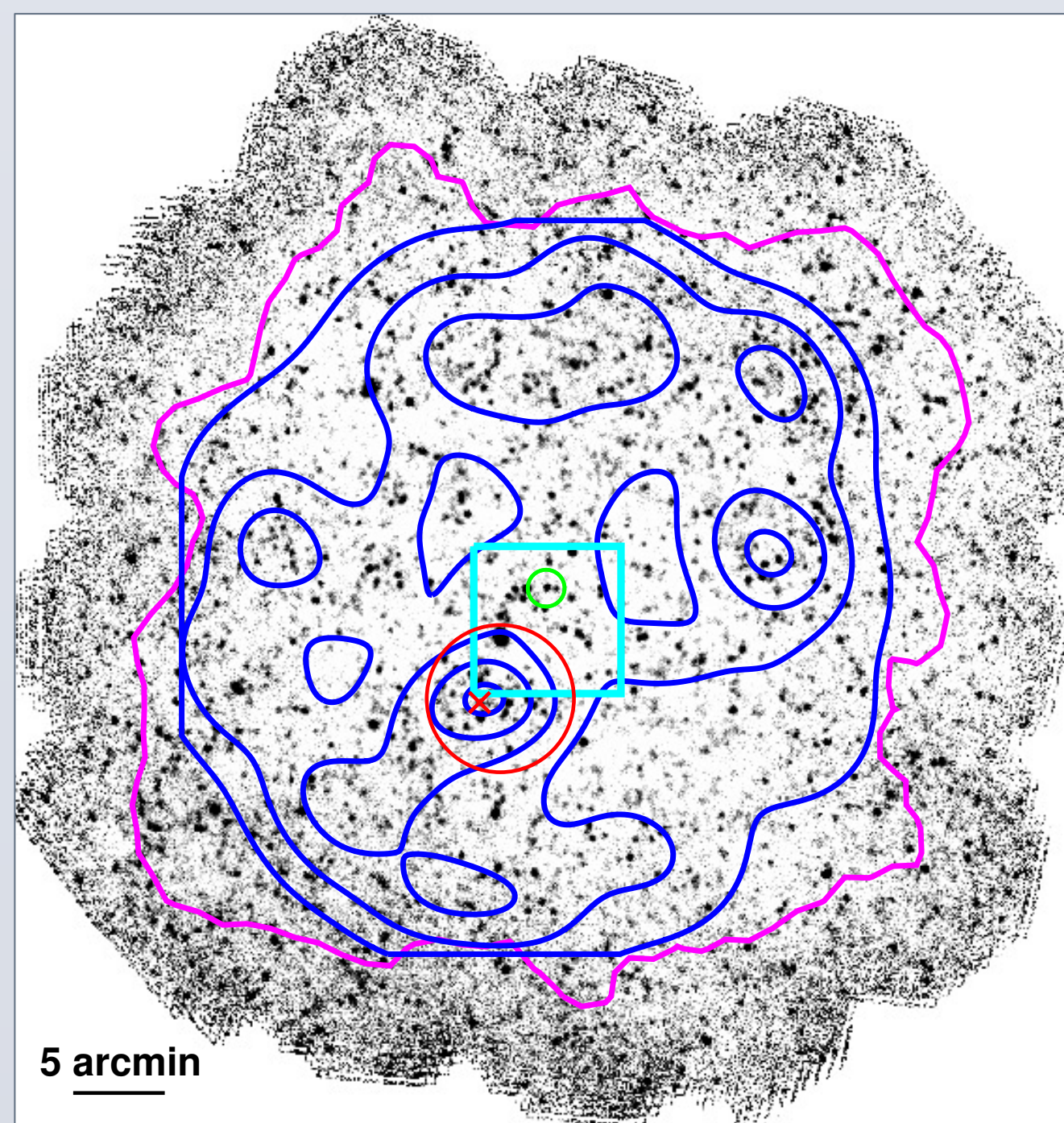


Fig.3 Combined SPiRE 250 μm GT1+OT2 map of the Spiderweb protocluster field. The green circle is the Spiderweb radio galaxy, red circle ($4'$ radius) is the overdensity region. The cyan box is the field from Fig.2. The magenta contour delineates the region of 50% coverage. The blue contours are the AKDE at 1 to 5σ

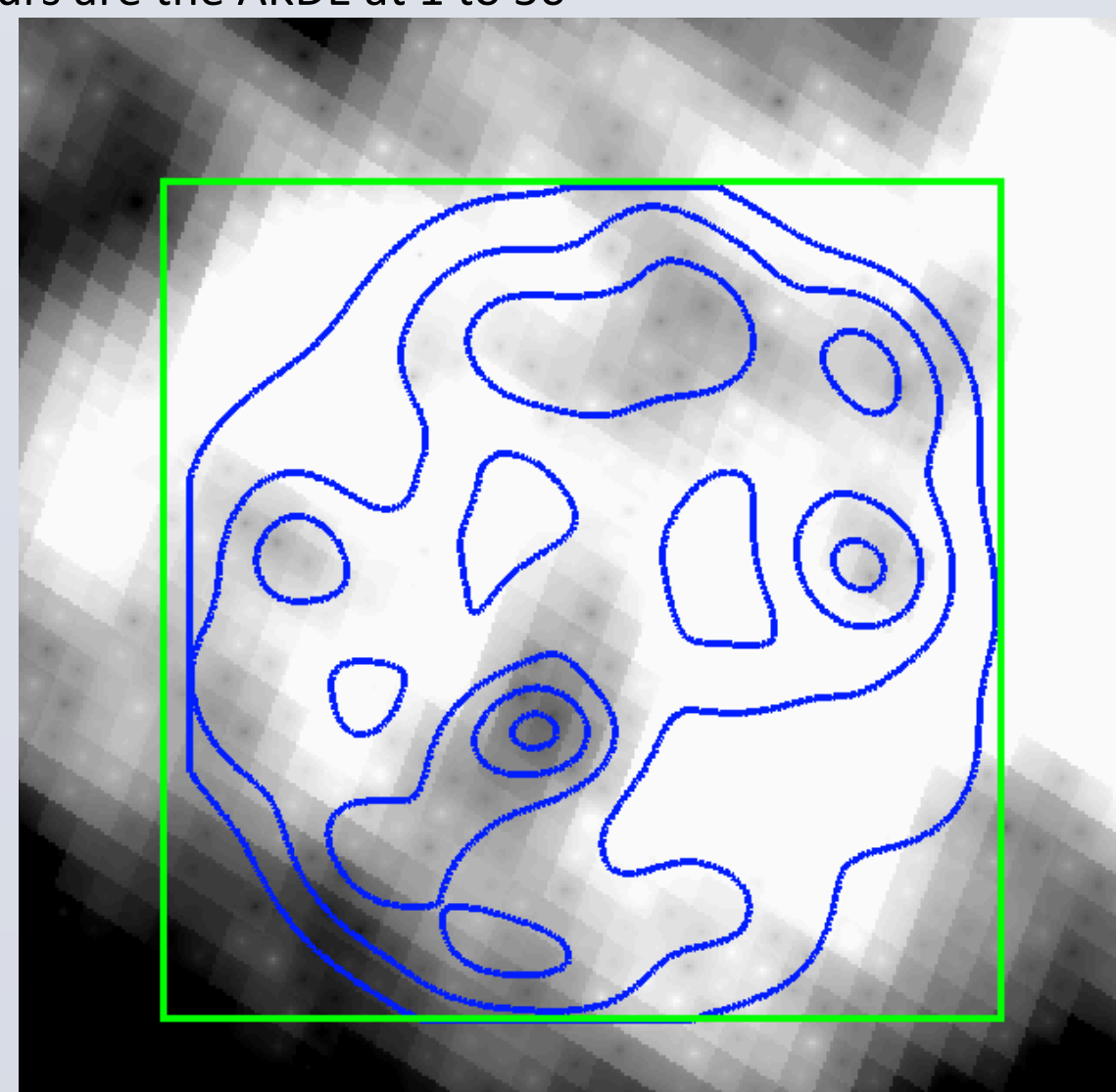


Fig.4 Planck/HFI 857 GHz map with the AKDE contours from Fig. 1. The green box is $40' \times 40'$, the peak flux in the overdensity is 2.56 MJy/sr.

Results

\Rightarrow Surface density excess

- \Rightarrow There are 76 (SNR > 3) 250 μm sources within the overdensity $\Rightarrow 1.51 \pm 0.17 \text{ arcmin}^{-2}$
- \Rightarrow There are 43 at S250 > 20 mJy $\Rightarrow 0.86 \pm 0.13 \text{ arcmin}^{-2}$
- \Rightarrow From control fields: $0.24 \pm 0.01 \text{ arcmin}^{-2}$ (or 12 ± 3 in a $4'$ radius) with S250 > 20 mJy. This is a factor of 3.6 excess of the overdensity vs the fields.
- \Rightarrow From control fields: in 1000 random regions of $4'$ radius max number of sources with S250 > 20 mJy are 42 in COSMOS, 35 in GOODS-North, 33 in UDS and 31 in Lockman, on average 20 ± 7 in $4'$ regions, still a factor of 2 excess.
- \Rightarrow Control fields: $4'$ regions with similar number of sources can be found, but they do not correspond to AKDE peak above $3.5\sigma \Rightarrow$ the overdensity is more centrally concentrated.

\Rightarrow Flux density distribution

- \Rightarrow The comparison from the S250 distribution from the control fields as well as with the number counts from Béthermin+12 indicates a marginal excess in the 30-40 mJy bin: we detect 8 sources while there are 4.4 ± 2.0 in the fields (and 4.3 ± 0.3 from Béthermin+12).

\Rightarrow FIR colours and blackbody redshifts

- \Rightarrow With at most 3 FIR photometric points the derivation of photo-z is challenging (e.g. Lapi+11, Roseboom+12, Casey12)
- \Rightarrow We fit a redshifted modified blackbody with a fixed dust temperature $T_d = 30 \text{ K}$ (eg Magnelli+12). Examples are shown in Fig. 6.
- \Rightarrow The best fit redshift zBB encapsulates the FIR colour information (S250/S350 and S350/S500) and the SED shape. zBB is very degenerate: $T_d/(1+z_{\text{BB}}) = \text{const} \Rightarrow$ changing the fixed T_d would change zBB.

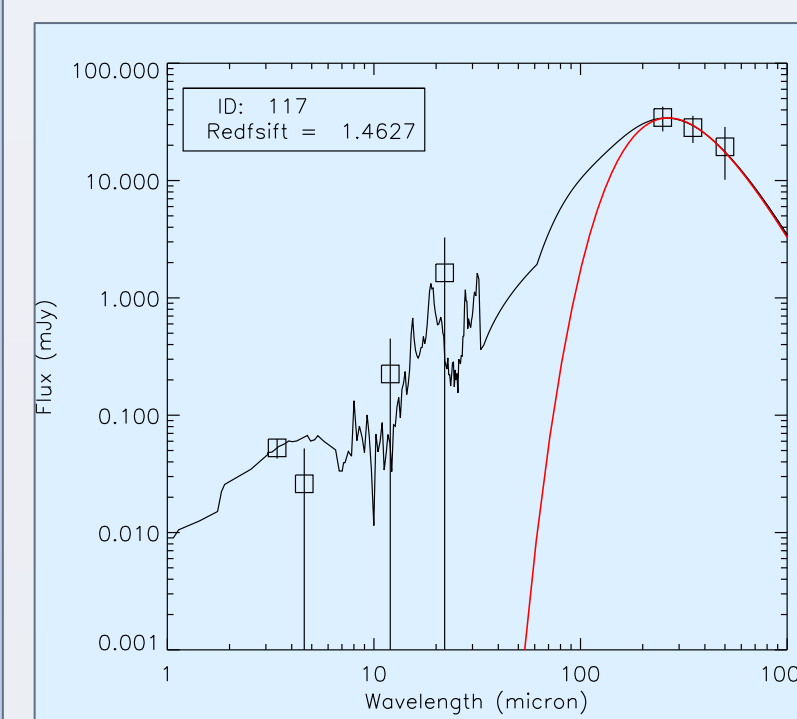


Fig. 6 Example of blackbody and SED fits. Upper panel source ID117 has WISE data.

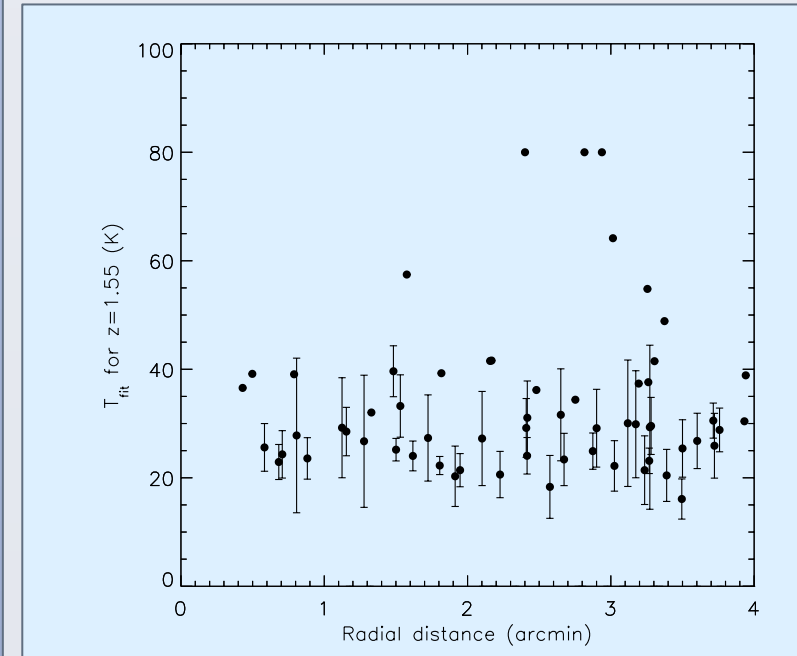


Fig. 10 Galaxy temperature distribution from the centre of the overdensity, for a fixed zBB redshift. No trend is seen.

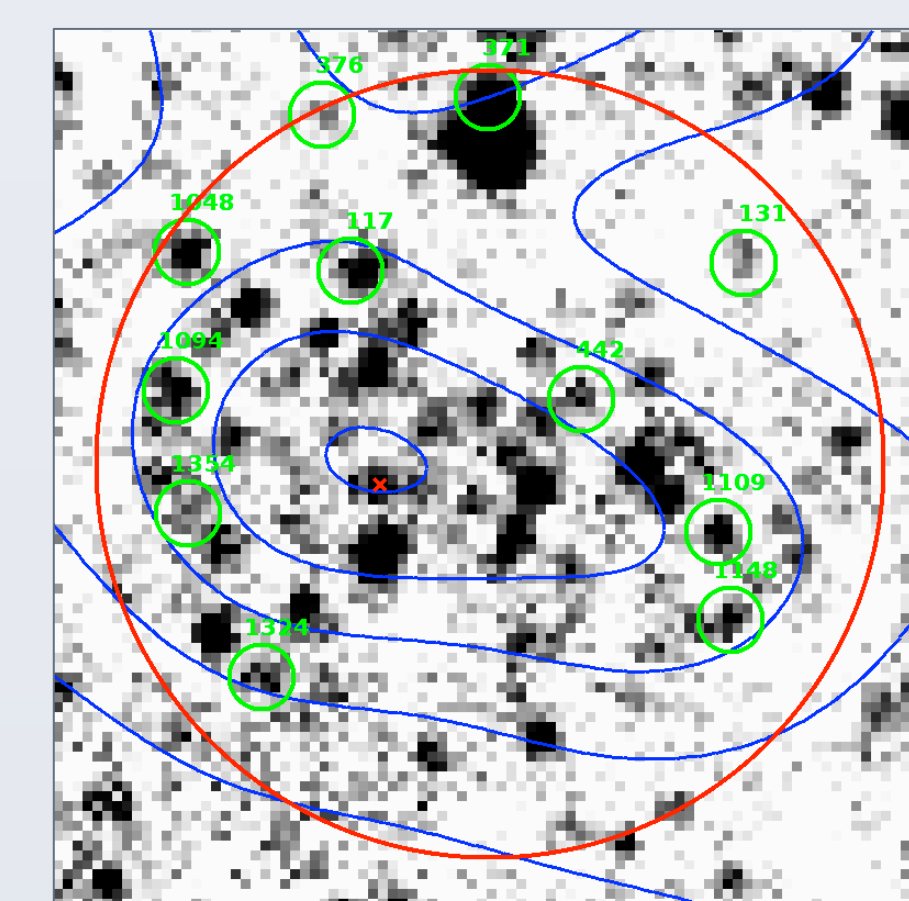


Fig. 9 Zoom on the overdensity. The sources with zBB in [1.45, 1.65] are marked with green circles.

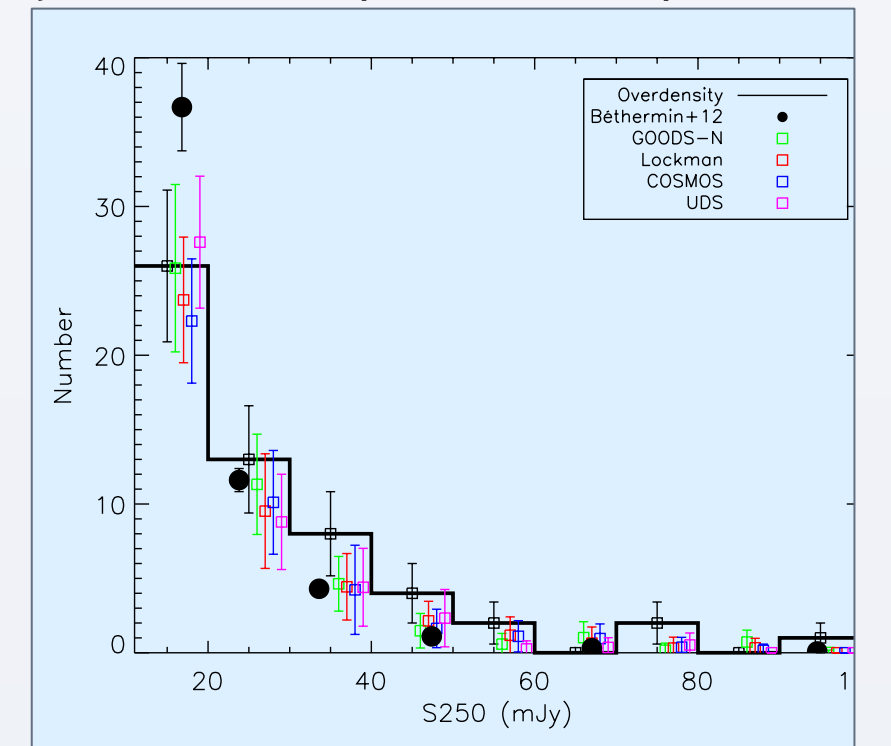


Fig.5 250 μm flux density distribution.

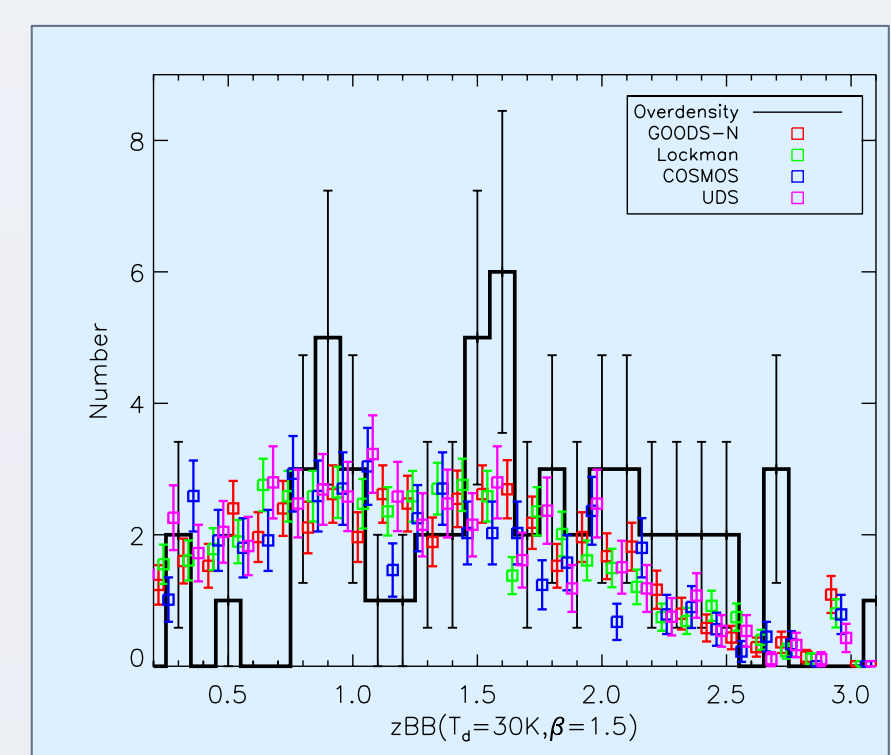


Fig. 7 Fitted zBB distributions (bin size is 0.1), errors are Poissonian.

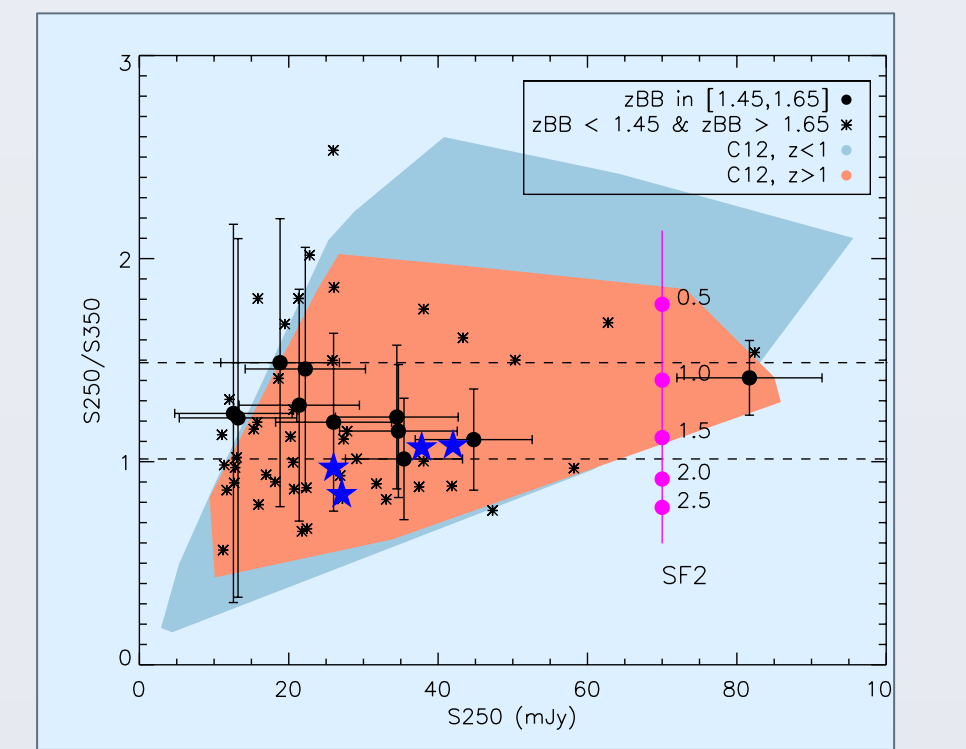


Fig. 8 Colour-magnitude diagram. The filled polygons delineate the regions occupied by Herschel galaxies with spectroscopic redshift from Casey+12 (C12). The track of a star-forming galaxy at different redshifts is shown in magenta. Filled circles with error bars are the sources with zBB in [1.45, 1.65]. Blue stars are Herschel-detected counterparts to spectroscopically confirmed Spiderweb galaxies at z=2.2 (Sánchez-Portal+, in prep)

Discussion and conclusions

\Rightarrow Serendipitous detection of a significant ($>5\sigma$) overdensity of 250 μm sources.

- \Rightarrow First report on such a discovery, more to come.
- \Rightarrow Herschel follow up of Planck sources revealed that some of them are also overdensities of sources (Clements+13), in 4 out of 16 Planck sources.
- \Rightarrow Detection of two overdensities in 26 fields around powerful radio galaxies (Rigby+13).

\Rightarrow No similar structures are identified in four wellknown extragalactic control fields.

\Rightarrow Similar AKDE peak occurs in 2 out of 100 simulated fields with randomly distributed sources (same number and same field geometry).

\Rightarrow Close to a known protocluster, at $\sim 7'$ south ($\sim 10 \text{ Mpc}$ comoving).

Q: can it be part of the protocluster complex?

- \Rightarrow If we fix T_d to 38 K then zBB peak will be at 2.2 (z- T_d degeneracy).
- \Rightarrow There is already a reported large-scale filament (10 Mpc comoving) North of the Spiderweb (Koyama+13), can this be a southern extension?

\Rightarrow Other possibilities:

- \Rightarrow Chance alignment of star-forming galaxies? But then the colours (by means of the zBB), the significant surface density excess and the space distribution are quite unusual \Leftarrow follow up needed.
- \Rightarrow Protocluster complex with no link to the Spiderweb \Leftarrow spectroscopy needed.

\Rightarrow Too scarce multi-wavelength data to make any strong statement but none of these hypotheses can be discarded with the currently available data. Follow-up needed to make any progress.

References:

- Béthermin, M. et al., 2012, A&A, 542, 58
 Cai, Z.-I., et al., 2013, ApJ, 768, 21
 Casey, C., 2012, MNRAS, 425, 3094
 Chapman, S. et al., 2009, ApJ, 691, 560
 Clements, D. et al., 2013, MNRAS submitted.
 Elbaz, D. et al., 2007, A&A, 468, 33
 Granato, G.L. et al., 2004, ApJ, 600, 580
 Hatch, N. et al., 2011, MNRAS, 415, 2993
 Hopkins A.M. & Beacom J.F., 2006, ApJ, 651, 142
 Kurk, J. et al., 2004a, A&A, 428, 793
 Kurk, J. et al., 2004b, A&A, 428, 817
 Koyama, Y. et al., 2013, MNRAS, 428, 1551
 Lapi, A. et al., 2011, ApJ, 742, 24
 Magnelli, B. et al., 2012, A&A, 539, 155
 Miley G. & De Breuck C., A&ARv, 15, 67
 Negrello, M. et al., 2005, MNRAS, 358, 869
 Nguyen, H. et al., 2010, A&A, 518, 15
 Oliver, S. et al., 2012, MNRAS, 424, 1614
 Pisani, A. 1996, MNRAS, 278, 697
 Popesso, P. et al., 2012, A&A, 537, 58
 Rigby, E. et al., 2013, MNRAS, in press
 Roseboom, I. et al., 2012, MNRAS, 419, 2758
 Seymour, N. et al., 2012, ApJ, 755, 146
 Smith, A.J. et al., 2012, MNRAS, 419, 377
 Stevens, J. et al., 2010, MNRAS, 405, 2623
 Takagi, T. et al., 1999, ApJ, 523, 107
 Wright, E.L. et al., 2010, AJ, 140, 1868

The paper on this overdensity will appear soon in MNRAS. The arXiv:1309.4223 PDF version is available with this QC

